

Polyhedral Oligomeric Silsesquioxane-Based Fluoroether-Containing Terpolymers: Synthesis, Characterization and Their Water and Oil Repellency Evaluation for Cotton Fabric

Yu Gao,^{1,2} Chuanglong He,² Feng-Ling Qing^{2,3}

¹Research Institute of Donghua University, Donghua University, Shanghai 201620, China

²College of Chemistry, Chemical Engineering and Biotechnology, Donghua University, Shanghai 201620, China

³Key Laboratory of Organofluorine Chemistry, Shanghai Institute of Organic Chemistry, Chinese Academy of Sciences, Shanghai 200032, China

Correspondence to: F.-L. Qing (E-mail: flq@mail.sioc.ac.cn)

Received 26 April 2011; accepted 16 August 2011; published online 30 September 2011

DOI: 10.1002/pola.24961

ABSTRACT: A series of polyhedral oligomeric silsesquioxane (POSS) based hybrid copolymers poly(POSS-co-methyl methacrylate-co-4-vinylbenzyl fluoroether carboxylate) (**P(POSS-MMA-VBFC)**) were prepared via radical polymerization and characterized by nuclear magnetic resonance, fourier transform infrared spectroscopy, thermogravimetric analysis, differential scanning calorimetry, gel permeation chromatography, X-ray powder diffraction, scanning electron microscopy and transmission electron microscopy. The thermal properties of these polymers ($T_d > 250$ °C) were improved by the introduction of POSS

cage. The cotton fabrics coated with the polymers possessed excellent water and oil repellency. The water and salad oil contact angle could be achieved from 133° to 159° and from 127° to 141° respectively as the content of POSS in the polymer increased from 0 to 7.1 wt %. Moreover, the cotton fabric coated with the terpolymer was less flammable than the uncoated one. © 2011 Wiley Periodicals, Inc. *J Polym Sci Part A: Polym Chem* 49: 5152–5161, 2011

KEYWORDS: copolymerization; fluoropolymers; nanocomposites; oil repellent; POSS; superhydrophobic

INTRODUCTION In the past decades, polyhedral oligomeric silsesquioxane (POSS)-incorporated polymer materials have attracted increasing interest due to their remarkable performance on the polymer matrix such as higher usage temperature, improved mechanical property, and enhanced fire retardation than their pristine counterpart.^{1–5} A variety of POSS-containing polymers including epoxy,^{6,7} poly(methyl methacrylate),^{8,9} polysiloxane,¹⁰ polyethylene,^{11,12} polypropylene,^{13,14} polystyrene,^{15,16} polynorbornene,^{17,18} and fluorine-containing polymers,^{19,20} have been prepared via blending or polymerization. Much attention has been focused on the thermal stability, oxidative resistance, mechanical properties, and flame retardancy of the POSS-based polymers. Recently, fluorinated POSS-containing long-chain fluoroalkyl groups blended with poly(methyl methacrylate) (PMMA) has been applied to fabricate water and oil repellent surface.^{21,22} Surfaces with water and oil repellency have been much concerned in diverse fields such as self-cleaning paint, sports and outdoor clothing, biomedical layers, integrated sensors, microfluidic channels, and so forth.^{23–26} It is demonstrated that the POSS-containing long-chain fluoroalkyl groups significantly increased the water and oil repellency of those materials. However, many studies suggested that molecules con-

taining perfluoroalkyl chain (C_nF_{2n+1} , $n \geq 8$) could accumulate in wildlife and human body, which result in a potential risk for human health and environmental concerns.^{27,28} Since 2000, the USA Environmental Protection Agency has taken various actions to help minimize the potential impact of long-chain perfluorinated chemicals on human health and the environment. Fluoropolyether has been proved no potential for irritation or skin sensitisation, no detectable genotoxic activity *in vitro* or *in vivo*, and no cardiac sensitization potential.²⁹ Fluoropolyether seems to be the promising substitute for long-chain perfluoroalkane due to their outstanding physical and chemical properties such as, high chemical resistance, high lubricating ability, low surface free energy, and low toxicity.^{29,30}

In our previous study,³¹ we found that the thermal property and water/oil repellency of the fluoroether-containing polymer could be improved by the introduction of POSS cages. Herein, we report the synthesis and characterization of another POSS-based semifluorinated poly(POSS-co-methyl methacrylate-co-4-vinylbenzyl fluoropolyether carboxylate) (**P(POSS-MMA-VBFC)**). The effects of POSS content on the thermal property, chemical structure, and morphology of the terpolymer are studied and the wettability and flammability

of the cotton fabric coated with the terpolymer are investigated as well. It is expected that P(POSS-MMA-VBFC) coated cotton fabric exhibit excellent water and oil repellency.

EXPERIMENTAL

Materials

Methyl methacrylate (MMA) was purchased from Sinopharm Chemical Reagent Co. (Shanghai, China) and distilled from calcium hydride under vacuum before use. 2,2'-azobisisobutyronitrile (AIBN) (Sinopharm Chemical Reagent Co., Shanghai, China) was recrystallized from methanol. Tetrahydrofuran (THF) (Sinopharm Chemical Reagent Co., Shanghai, China) was distilled from sodium/benzophenone immediately before use. Octavinyl polyhedral oligomeric silsesquioxane (Ov-POSS) (99%) was purchased from Shenyang Meixi Fine Chemicals Co. (Shenyang, China) and dried under vacuum before use. Lithium aluminium hydride was purchased from Sigma-Aldrich Shanghai Trading Co. (Shanghai, China). 1-(chloromethyl)-4-vinylbenzene was purchased from J&K Scientific (Beijing, China). 2,3,3,3-tetrafluoro-2-(1,1,2,3,3,3-hexafluoro-2-(perfluoropropoxy)propoxy)propanoyl fluoride (THPF) was obtained from Shanghai Institute of Organic Chemistry, Chinese Academy of Sciences. All other chemicals were purchased from Sinopharm Chemical Reagent Co. (Shanghai, China) and used as received.

Measurements

^1H , ^{19}F , and ^{29}Si NMR spectra were recorded at ambient temperature on Bruker AV400 operating at 400.0, 376.4, and 79.6 MHz, respectively. Tetramethylsilane was applied as the internal chemical shift reference for ^1H NMR, and CDF_3 as external standard for ^{19}F NMR. Infrared spectra were recorded on a fourier transform infrared (FTIR) spectrometer (Avatar 380) using KBr crystal in the infrared region $4,000\text{--}400\text{ cm}^{-1}$. Gel permeation chromatography (GPC) analysis was carried out in THF at $35\text{ }^\circ\text{C}$ with a flow rate of 1.0 mL/min using a Waters 1515 system fitted with Waters 2414 differential refractive index detector. THF was used as eluent and the system was calibrated with polystyrene standards. Differential scanning calorimetry (DSC) was performed under N_2 atmosphere with a heating rate of $10\text{ }^\circ\text{C/min}$ on a Netzsch DSC 204 F1 Phoenix. Thermogravimetric analysis (TGA) was carried out under N_2 atmosphere with a heating rate of $10\text{ }^\circ\text{C/min}$ up to $800\text{ }^\circ\text{C}$ by using a Netzsch TG 209 F1 instruments. X-ray powder diffraction (XRD) patterns of the polymers were recorded using an X-ray diffractometer (PW 1830, Philips, Netherlands) with $\text{Cu K}\alpha$ Ni-filtered radiation at 2θ ranging from 5 to 60° in steps of 0.02° . Transmission electron microscopy (TEM) and scanning electron microscopy (SEM) images were obtained using Hitachi H-800 transmission electron microscope and JEOL JSM-5600LV scanning electron microscope, respectively. TEM samples were prepared by dip coating carbon coated copper grids with polymer solutions. SEM samples were prepared by drop coating the polymer solutions in THF (10 mg/mL) on cleaned slide glasses. The sessile drop method was used for static contact angle measurements at ambient temperature with an automatic video contact-angle testing apparatus

(DataPhysics OCA 40, DataPhysics Instruments GmbH; Germany). The probe liquids were deionized water, salad oil, and hexadecane. The average contact angle (CA) value was determined by measuring three to five different positions of the same sample with $5\text{ }\mu\text{L}$ probe liquid each time.

Synthesis

Synthesis of (4-Vinylphenyl)methanol (1)

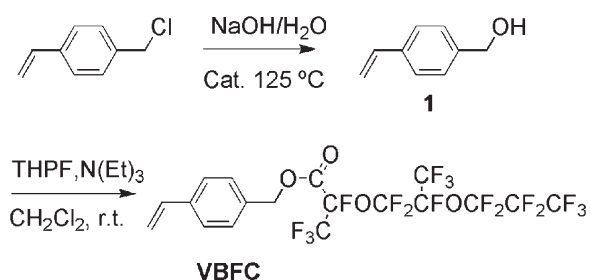
(4-vinylphenyl)methanol (**1**) could be obtained via hydrolysis of 1-(chloromethyl)-4-vinylbenzene in NaOH aqueous solution with phase-transfer catalyst³² (Scheme 1). In a typical synthesis, NaOH (0.08 g, 2 mmol) and N-hexadecyltrimethylammonium bromide (7.3 g, 20 mmol) were dissolved in distilled water (100 mL), and then 1-(chloromethyl)-4-vinylbenzene (3.0 g, 20 mmol) was added. The mixture was stirred at $125\text{ }^\circ\text{C}$ for 40 min, subsequently cooled to room temperature and extracted with ethyl acetate ($80\text{ mL} \times 3$). The combined organic layers were dried with anhydrous MgSO_4 , and then filtered. The resulting liquid was concentrated and purified by column chromatography using ethyl acetate-petroleum ether (v/v, 1:5) to give **1** as colorless oil with yield of 95% (2.5 g).

^1H NMR (CDCl_3 , 400.0 MHz, ppm): 1.85 (s, 1H, O—H), 4.58 (s, 2H, $\text{C}_6\text{H}_4\text{CH}_2\text{O}$), 5.17 (d, $J = 10.9\text{ Hz}$, 1H, $\text{CH}=\text{CHC}_6\text{H}_4$), 5.67 (d, $J = 17.6\text{ Hz}$, 1H, $\text{CH}=\text{CHC}_6\text{H}_4$), 6.64 (dd, $J = 17.6, 10.9\text{ Hz}$, 1H, $\text{CH}_2=\text{CHC}_6\text{H}_4$), 7.23 (d, $J = 8.0\text{ Hz}$, 2H, C_6H_4), 7.32 (d, $J = 8.0\text{ Hz}$, 2H, C_6H_4). IR (ν_{max} , cm^{-1} , KBr): 3,334 (O—H, broad), 3,086 and 2,872 (C—H), 1,629 (C=C), 1,512 (C—C of Ar).

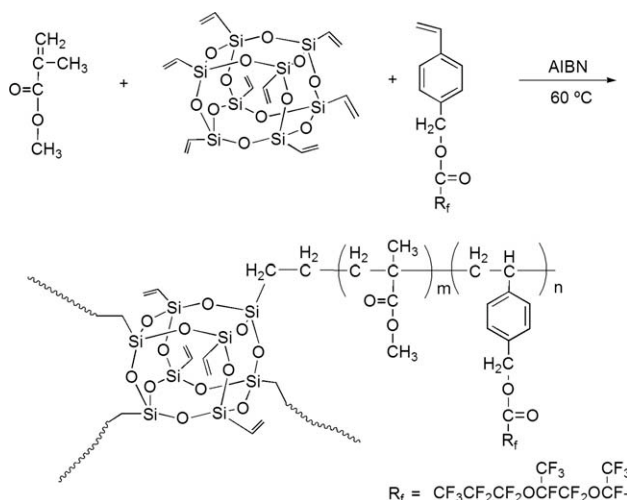
Synthesis of 4-Vinylbenzyl Fluoroether Carboxylate (VBFC)

To a dry three-necked flask fitted with condenser, dry dichloromethane (50 mL) and **1** (4.5 g, 34 mmol) were added followed by triethylamine (3.4 g, 34 mmol). Then THPF (16.8 g, 34 mmol) was slowly added dropwise at $-20\text{ }^\circ\text{C}$ under N_2 . After addition of THPF, the mixture was stirred at room temperature for 2 h. Subsequently, the reaction was quenched with a few drops of water. The mixture was then washed with water ($30\text{ mL} \times 3$) and dried with anhydrous MgSO_4 , and then filtered, concentrated, and purified by column chromatography using ethyl acetate-petroleum ether (v/v, 1:20) to give **VBFC** (see Scheme 1 for its chemical structure) as colorless oil with yield of 91% (18.6 g).

^1H NMR (CDCl_3 , 400.0 MHz, ppm): 4.53 (s, 2H, $\text{C}_6\text{H}_4\text{CH}_2\text{O}$), 5.23 (d, $J = 11.2\text{ Hz}$, 1H, $\text{CH}=\text{CHC}_6\text{H}_4$), 5.74 (d, $J = 17.6\text{ Hz}$, 1H, $\text{CH}=\text{CHC}_6\text{H}_4$), 6.71 (dd, $J = 11.2, 17.6\text{ Hz}$, 1H,



SCHEME 1 Synthesis of 4-vinylbenzyl fluoroether carboxylate (VBFC).



SCHEME 2 Preparation of P(POSS-MMA-VBFC).

$\text{CH}_2=\text{CHC}_6\text{H}_4$), 7.32 (d, $J = 8.0$ Hz, 2H, C_6H_4), 7.40 (d, $J = 8.0$ Hz, 2H, C_6H_4). ^{19}F NMR (CDCl_3 , 376.4 MHz, ppm): -145.2 (m, 1F, $\text{OCF}_2\text{CF}(\text{CF}_3)$), -131.5 (m, 1F, $\text{CF}(\text{CF}_3)\text{C}=\text{O}$), -129.7 (m, 2F, $\text{OCF}_2\text{CF}_2\text{CF}_3$), -84.7 to -79.4 (m, 13F, all OCF_2 and CF_3 signals). IR (ν_{max} , cm^{-1} , KBr): 3093 and 3015 (C–H), 1785 (C=O), 1638 (C=C), 1332 and 1240 (C–F), 1144, 1038 and 993 (C–O–C).

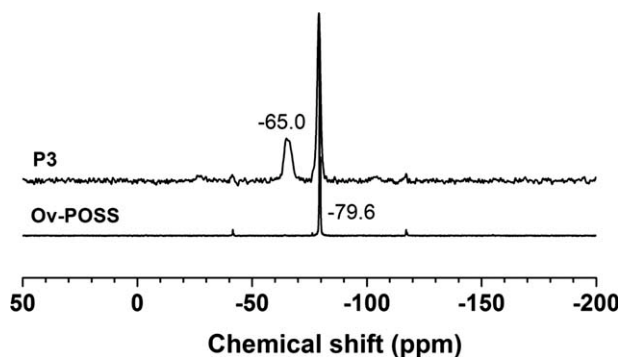
Synthesis of Terpolymer P(POSS-MMA-VBFC)

In a typical polymerization procedure, to a three-necked flask fitted with condenser and N_2 inlet, THF (5 mL), MMA (0.3 g, 3 mmol), VBFC (0.9 g, 1.5 mmol) and Ov-POSS at desired amount were added, followed by 1 wt % AIBN relative to monomers. The solution was allowed to stir at 60 °C for 24 h, followed by dropwise addition into a 10-fold excess of chloroform/methanol (v/v, 1:30) under vigorously agitation. The precipitate was then filtered and redissolved in chloroform and reprecipitated in chloroform/methanol (v/v, 1:30). This purification procedure was repeated at least three times. The polymers were finally dried at 50 °C under vacuum to give a white powder with constant weight. The polymers with different POSS feed amount of 0, 0.05, 0.1, 0.15 g were labeled by **P1**, **P2**, **P3**, **P4**, respectively. The synthesis of the terpolymer is outlined in Scheme 2.

^1H NMR (CDCl_3 , 400.0 MHz, ppm): 0.3–2.3 (m, CH_2 , CH_3 in backbone), 2.8 (s, CHC_6H_4), 3.6 (m, OCH_3), 5.3 (s, $\text{C}_6\text{H}_4\text{CH}_2\text{O}$), 5.8–6.2 (m, $\text{CH}_2=\text{CHSi}$), 6.5–7.3 (m, C_6H_4). ^{29}Si NMR (solid, 79.6 MHz, ppm): -79.6 ($\text{Si}-\text{CH}_2$), -65.0 ($\text{Si}-\text{CH}$). IR (ν_{max} , cm^{-1} , KBr): 3,000–2,900 (C–H), 1785 and 1734 (C=O), 1240 (C–F), 1,143 (C–O–C), 1109 and 583 (Si–O–Si).

Treatment of the Cotton Fabric with the Polymers

The desized, bleached, and cleaned cotton fabrics (3 cm × 10 cm) were soaked in the 0.01 g/mL polymers solution (THF as solvent) for 2 h. The cotton fabrics were dried at 80 °C for 30 min and then cured at 160 °C for 3 min. The cotton fabrics coated with **P1**, **P2**, **P3** were labeled by **S1**, **S2**, **S3**, respectively.

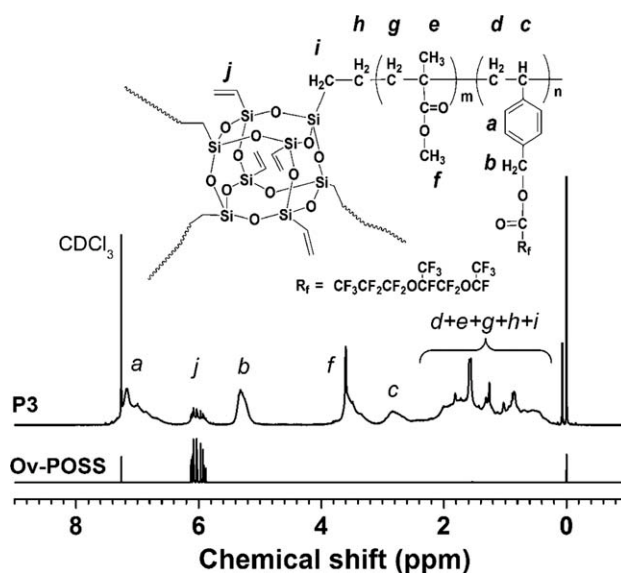
FIGURE 1 ^{29}Si NMR spectra of Ov-POSS and **P3**.

RESULTS AND DISCUSSION

Chemical Characterization

The terpolymer P(POSS-MMA-VBFC) was synthesized by conventional radical polymerization. When the product solution was added in a chloroform/methanol (v/v, 1:30) solution dropwise, the desired polymer P(POSS-MMA-VBFC) was precipitated instead of Ov-POSS. Such dissolution-precipitation procedure was repeated at least three times to remove the unreacted Ov-POSS.

The chemical composite of the polymer P(POSS-MMA-VBFC) was characterized by NMR and FTIR. Figure 1 shows the solid-state ^{29}Si NMR spectra of Ov-POSS and P(POSS-MMA-VBFC). The signal at -79.6 ppm in ^{29}Si NMR spectrum of Ov-POSS is assigned to silicon atoms connected to the vinyl group. In ^{29}Si NMR spectrum of P(POSS-MMA-VBFC) (**P3**), the appearance of a new signal at -65.0 ppm indicates that Ov-POSS participated in the polymerization. The ^1H NMR spectra of Ov-POSS and P(POSS-MMA-VBFC) (**P3**) in *d*-chloroform were shown in Figure 2. For pure Ov-POSS, the multiple resonance peaks of vinyl protons are observed in the region of 5.8–6.2 ppm. For P(POSS-MMA-VBFC), the

FIGURE 2 ^1H NMR spectra of Ov-POSS and **P3**.

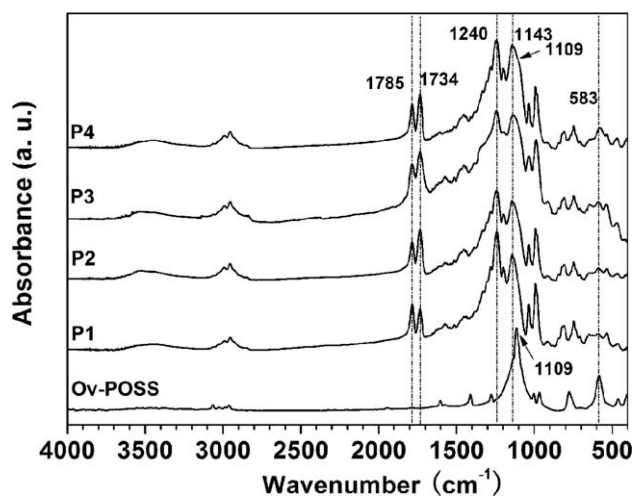


FIGURE 3 FTIR spectra of Ov-POSS and P(POSS-MMA-VBFC) with different Ov-POSS wt % ratio. (**P1**: 0, **P2**: 3.2, **P3**: 7.1, **P4**:10.8).

signals **a** in the region of 6.5–7.3 ppm, **b** at ~5.3 ppm and **c** at ~2.8 ppm are assigned to the aromatic protons, benzyloxy protons and methenyl protons of VBFC unit, respectively. The signal **f** at ~3.6 ppm is attributed to methyl protons connected to ester group in MMA unit. The resonance peaks in the region of 0.3–2.3 ppm are the overlapping proton signals of methylene groups in the terpolymer backbone and the side methyl groups in MMA unit. The weak peak at ~6.0 ppm indicates the existence of unreacted vinyl group in Ov-POSS segment, which is consistent with the result from ²⁹Si NMR. The number of reacted vinyl groups of all the terpolymers ranged from 4.0 to 4.3 calculated according to the data of elemental analyses of Si and ¹H NMR. The residue vinyl groups provide an opportunity for introducing other functional groups into the terpolymers in further applications.

The chemical structure of the terpolymer is confirmed by FTIR spectra of **P2**, **P3** and **P4** in Figure 3. FTIR spectra of P(MMA-VBFC) (**P1**) as well as the pure Ov-POSS for comparison are also presented in Figure 3. For neat Ov-POSS, the strong absorption bands at ~1109 and 583 cm⁻¹ are due to the characteristic Si–O–Si stretching vibration of silsesquioxane cages. The spectra of **P2–P4** show the relative

peak broadening at ~1,109 cm⁻¹ with the increase of POSS content in the terpolymer. Moreover, the intensity of the peak at 583 cm⁻¹ also increases with increasing POSS content in the terpolymer, indicating that the POSS cages probably have been incorporated into the polymeric chains. For **P1–P4**, the characteristic bands at ~1,785, ~1,734 cm⁻¹ are assigned to carbonyl group in VBFC and MMA unit, respectively, while the bands at ~1,240 and ~1,143 cm⁻¹ are attributed to C–F and C–O–C groups. The stretching absorption bands of –CH₂ and –CH₃ groups in the polymers are located at 3,000–2,900 cm⁻¹. The NMR and FTIR analysis verified the successful synthesis of P(POSS-MMA-VBFC).

The polymers **P1**, **P2**, and **P3** show good solubility in THF, chloroform and dichloromethane, while **P4** with POSS content of 10.8 wt % is insoluble in common organic solvents. So the molecular weights (*M_w* and *M_n*) of the polymers except **P4** were measured by GPC and summarized in Table 1. The yield and *M_w* of the polymer without POSS (**P1**) is 78% and 57 × 10³ g/mol, respectively, while they are decreased to 62% and 6.8 × 10³ g/mol, when the polymer containing 7.1 wt % POSS segments (**P3**). It is obvious that the yields or molecular weights of products decrease with the increase of POSS contents, which is consistent with the result of our previous work³¹ and Xu's work.^{33,34} Among MMA, VBFC, and POSS, we think that the least reactive and stable free radical is POSS free radical due to the strong steric hindrance effect from the bulky POSS group.³⁴ Thus, MMA and VBFC would be easier to be initiated by AIBN, and P(MMA-VBFC) free radicals would be formed first. Once the propagating P(MMA-VBFC) radicals combined with POSS free radicals, the chain termination would occur, generating the star-shaped polymers rather than the network ones. With the increase of POSS content, the probability for the collision between the propagating P(MMA-VBFC) free radicals and POSS free radicals increased, resulting P(MMA-VBFC) chains were shorter when the chain termination occurred, as a result, the lower molecule weight and yield of the terpolymers (**P2**, **P3**) were obtained. The steric hindrance effects from bulky POSS group on molecule weight or reaction conversions of polymer have also been reported by Kim and Chujo³⁵ and Liu and Lee.³⁶ **P2** and **P3** exhibiting good solubility proved that they were star-shaped or low crosslinking structures rather than large network structure since network

TABLE 1 Effects of POSS Content on Yield, Molecular Weight and Thermal Properties of P(POSS-MMA-BVFC)

Samples	POSS (wt %)		Yield (%)	<i>M_w</i> (×10 ³ g/mol)	PDI (<i>M_w</i> / <i>M_n</i>)	<i>T_g</i> (°C)	<i>T_{d5}</i> ^b (°C)	Residue Char ^c (%)
	Feed ratio	Product ratio ^a						
P1	0	0	78.3	57	2.5	28.6	249	3.9
P2	4.0	3.2	75.8	9.0	1.2	42.2	267	7.5
P3	7.7	7.1	62.3	6.8	1.3	48.0	274	12.2
P4	11.1	10.8	65.2	-	-	50.2	276	16.2

^a Calculated from the elemental analyses of Si.

^b Temperature at weight loss of 5 %.

^c Obtained from TGA.

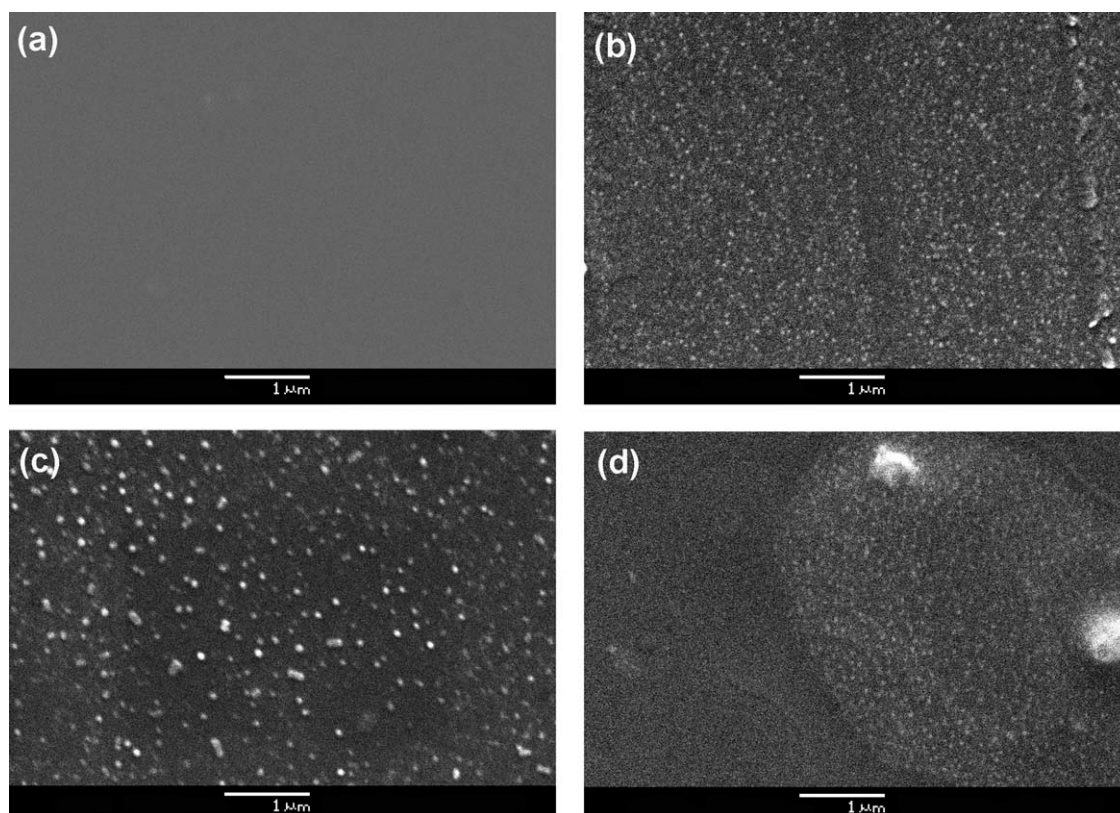


FIGURE 4 SEM images of **P1**(a), **P2**(b), **P3**(c), and **P4**(d).

polymers are hardly soluble in any solvents.³⁴ However, with excessive POSS content (e.g., 10.8 wt %), the crosslinking reactions between two propagating POSS-based free radicals would occur and thus facilitate the formation of polymer networks, resulting in a relative poor solubility of **P4**.

Structure and Morphology

Figures 4 and 5 show the SEM and TEM images of the polymers. **P1**, **P2**, and **P3** were soluble in THF, so the uniform films were obtained on the substrate [Fig. 4(a–c)]. In Figure 4(d), the area covered by numerous small and two big white pots is **P4** sample, which was insoluble and only swelled in THF. The SEM image of **P1** [Fig. 4(a)] exhibit homogeneous morphology without localized domains because there was no POSS incorporated into **P1**. The white pots in Figure 4(b–d)

correspond to POSS agglomerates in **P2**, **P3**, and **P4**. In TEM images, the dark pots are POSS agglomerates. Both SEM and TEM images show that between the POSS agglomerates in **P2** and **P3**, the latter are bigger in size. It shows that the size of POSS agglomerates increases with the increasing of POSS content in the terpolymer. In the TEM image of **P4** sample [Fig. 5(d)], the network with dark pots revealed the swelled polymer was network and imbedded with POSS agglomerates.

As seen in Figure 4, POSS segments exist in **P2** and **P3** as nano agglomerates and take good dispersion without crystalline aggregates. This result agrees with the XRD patterns of the polymers, as shown in Figure 6. The Ov-POSS is a highly crystalline material and has a characteristic dominant

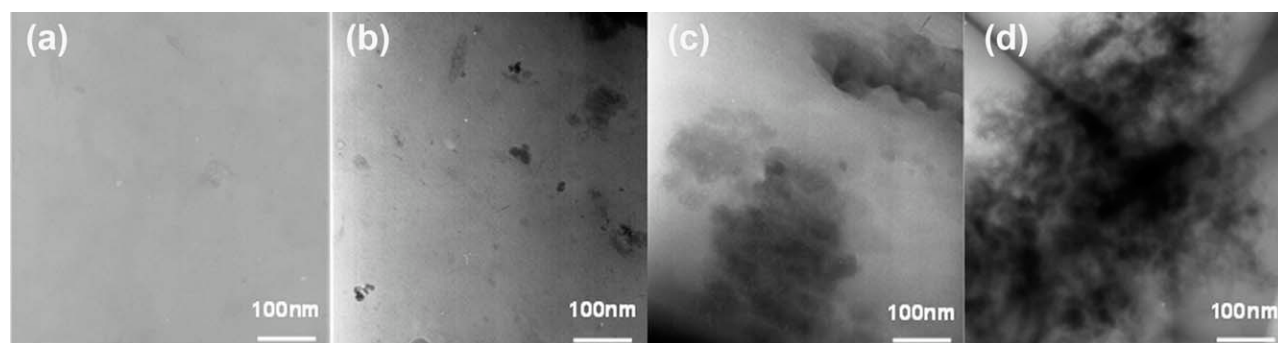


FIGURE 5 TEM images of **P1**(a), **P2**(b), **P3**(c), and **P4**(d).

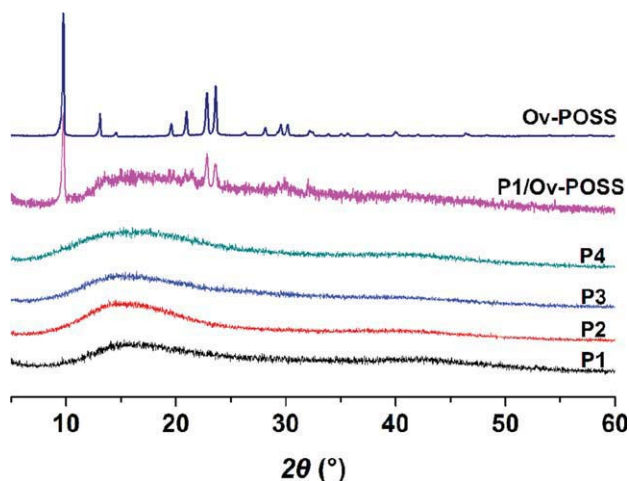


FIGURE 6 XRD patterns of the polymers.

diffraction peak at $2\theta = 9.7^\circ$.³⁷ In the **P1/Ov-POSS** physical blending (5 wt % Ov-POSS), the peak corresponding to the dominant Ov-POSS peak appears, indicating the presence of Ov-POSS crystalline aggregates in the polymer matrix. It is noted that the XRD patterns of **P2**, **P3**, and **P4** exhibit amorphous structure without any peaks corresponding to Ov-POSS crystalline, indicating POSS exist in the terpolymers as polymer segments without crystalline aggregates due to the obstruction of the polymer chains around the POSS core to the POSS crystal structure formation. Based on the above results, the structure of the terpolymer P(POSS-MMA-VBFC) with different POSS content is proposed as Figure 7. The terpolymers with low POSS content were probably star-shaped structure [Fig. 7(a)], while the terpolymers with high POSS content were crosslinked network [Fig. 7(b)].

Thermal Properties

The influence of POSS on the thermal behavior of the polymers is evaluated by means of TGA and DSC. Figure 8(a) shows the weight loss of polymers when heated from ambient temperature ($\sim 25^\circ\text{C}$) to 800°C under a nitrogen flow at a heating rate of $10^\circ\text{C}/\text{min}$. The TGA curves are characterized as two stage decomposition which could be attributed to the degradation of backbone ($300\text{--}400^\circ\text{C}$) and the

elimination of phenyl ring ($400\text{--}500^\circ\text{C}$), respectively. The decomposition temperatures for 5% weight loss (T_{d5}) of the polymers with TGA are found to be 249°C for **P1**, 267°C for **P2**, 274°C for **P3** and 276°C for **P4**, which shows that T_{d5} rises with the increase of POSS content. Moreover, the residue char weight increased from 3.9 to 16.2 wt % when POSS content increase from 0 to 10.8%, as seen in Figure 8(a) and Table 1. The peak temperatures at which velocity of weight loss reaches maximum (T_m) are displayed in DTG curves [Fig. 8(b)]. As seen from **P1** to **P4** in Figure 8(b), T_m rises from 349 to 371°C when POSS content increase from 0 to 10.8%. This indicates clearly that incorporation of POSS is beneficial for improving the thermal stability of the polymer.

The glass transition temperature (T_g) of the polymers is displayed in Table 1. The T_g of **P1** is only 28.6°C , but that of **P4** up to 50.4°C . It is obvious that the incorporation of POSS cage structure into P(MMA-VBFC) results in dramatic T_g increases, which is consistent with the results from Liu and Zheng³⁸ and Yang et al.³⁹ The reason for T_g improvement is probably that the POSS segments dispersed in the terpolymer hindering the motion of P(MMA-VBFC) chains in the polymer matrix.

Surface Morphology of the Coated Cotton Fabrics

The surface morphology of the cotton fabric treated with **P1**, **P2**, or **P3** before and after is shown in Figure 9. The uncoated cotton fiber surface shows the natural texture with some irregular grooves [Fig. 9(a)]. When the cotton fabric is coated with **P1**, the surface of **S1** becomes relative smooth due to the polymer filling in the grooves [Fig. 9(b)]. As shown in Figure 9(c,d), in the SEM images of **S2** and **S3**, no POSS crystal aggregates are present, but some white dots caused by POSS agglomeration are observed, which is consistent with the SEM images of the corresponding terpolymers. The surface of **S1** [Fig. 9(b)] has no such white dots because of the absence of POSS unit in **P1**. Compared with **S1**, the SEM and AFM (Fig. 10) images of **S2** or **S3** show rougher surface due to POSS agglomeration in the terpolymers.

Wettability of the Coated Fabrics

The wettability of the coated cotton fabric surface was assessed through water and oil contact angle measurements. The corresponding contact angles of the coated cotton fabric

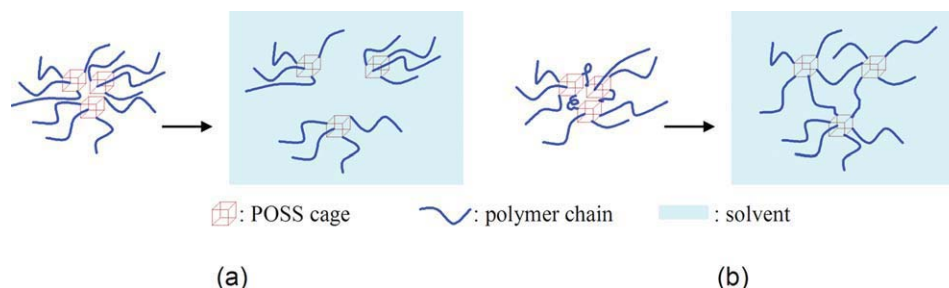


FIGURE 7 Schematic microstructures of POSS-based terpolymer with low (a) or high (b) POSS content.

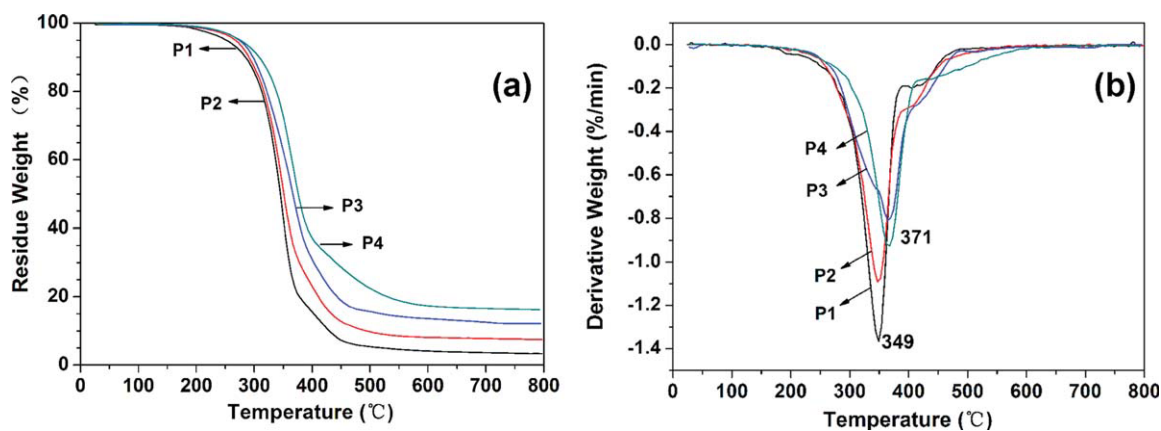


FIGURE 8 TGA (a) and DTG (b) curves of polymers under nitrogen.

samples are given in Table 2. The water images on the samples during water CA measurement are shown as insets of Figure 9. The observed water CA of **S1** which was coated with non-POSS containing polymer is only $\sim 133^\circ$, much lower than that of **S2** and **S3** which were coated with POSS-based polymers. When the POSS content in the polymer is from 3.2 to 7.1%, the water CA of the coated cotton fabrics increases from $\sim 143^\circ$ (**S2**) to $\sim 159^\circ$ (**S3**). The data summarized in Table 2 show that water CA increases with the increasing of POSS content, which indicates that hydrophobicity of the coated cotton fabrics were improved by the addition of POSS. When the POSS content in the POSS-based

polymer is up to 7.1%, on the polymer coated cotton fabrics (**S3**), the water CA is higher than 150° and the CA hysteresis is lower than 5° , achieving superhydrophobicity. Similarly, the salad oil CAs of samples **S1**, **S2**, and **S3** ($\sim 127^\circ$, $\sim 132^\circ$, and $\sim 141^\circ$) indicate that the salad oil repellency is also improved by the incorporation of POSS in the coating polymer.

By contrast, for the lower surface tension oil, hexadecane (surface tension: 27.4 mN/m, 20 °C), the CAs on the polymer coated samples (**S1**, **S2**, and **S3**) are $\sim 121^\circ$, $\sim 128^\circ$, and $\sim 110^\circ$, respectively. With the increase of the POSS content from 3.2 to 7.1% in the POSS-based polymer, the hexadecane

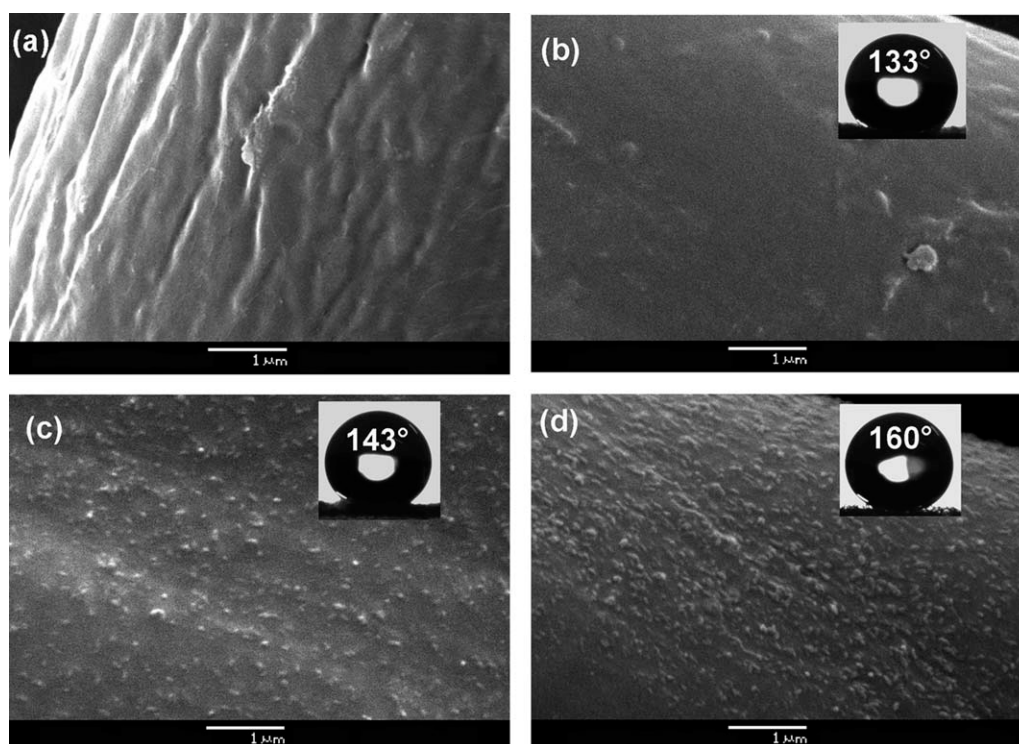


FIGURE 9 SEM images of the surfaces of uncoated fabric (a), **S1** (b), **S2** (c), and **S3** (d). Insets are photos of water droplets on the corresponding samples.

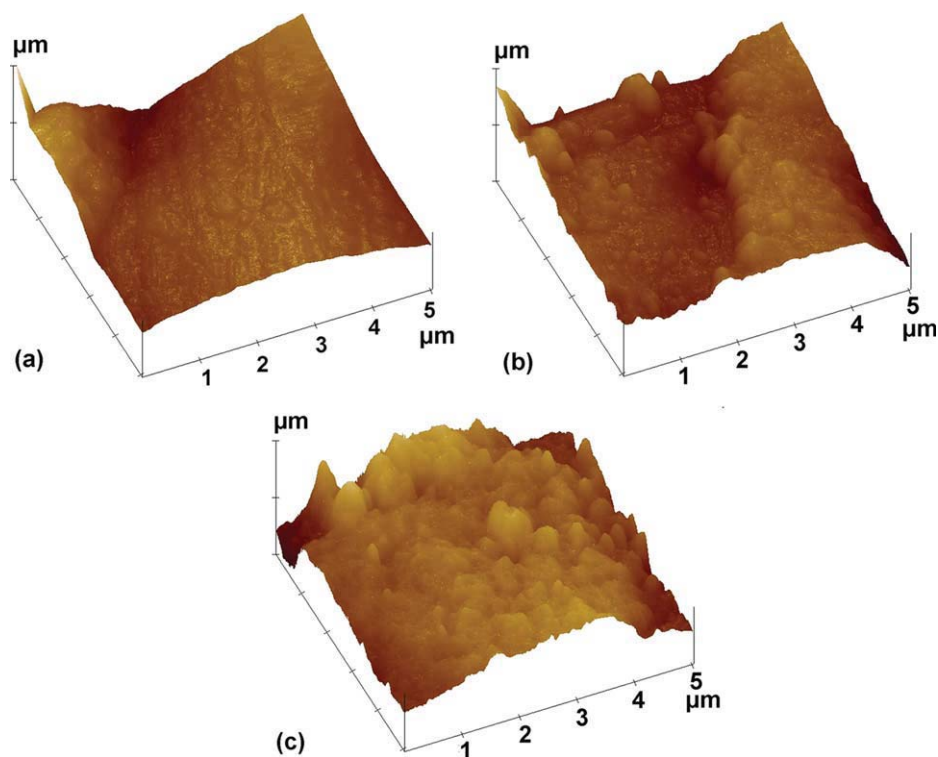


FIGURE 10 AFM images of **S1** (a), **S2** (b), and **S3** (c).

CA on the coated samples doesn't increase but decreased from $\sim 128^\circ$ (**S2**) to $\sim 110^\circ$ (**S3**).

Such effect of POSS content on water and oil repellency of the coated cotton fabrics is similar to the result of our previous work.³¹ The liquid repellency of the surface is determined by both the surface chemical composite and the surface morphology. The surface with appropriate roughness and low enough surface free energy could realize superhydrophobicity and highly oleophobicity or even superoleophobicity. In this study, the POSS content in the coating polymer influences both the surface free energy and the roughness. With the increase of POSS content, the surface roughness increases because of POSS agglomeration, and the surface free energy also increases due to the inevitable decrease of fluorine content in the polymer. For liquids with high surface tension, e.g., water, the morphology of hydrophobic solid surface is the decision factor to achieve superhydrophobicity. Therefore, among the coated cotton fabrics samples, the water CA of **S3** is much higher than that of **S2** and **S1** because of the roughest surface morphology of **S3**. The common household liquids existing as ball-like droplet on **S3** and as stain spot on the uncoated cotton fabrics surface are shown in Figure 11, which indicates the antifouling ability of the cotton fabric is improved significantly by the POSS-based fluoroether-containing polymer coating. When the coated cotton fabrics contact with the liquids with low surface tension, e.g., hexadecane, higher fluorine content in their coatings is needed to achieve a lower surface free energy of the coated surface and thus renders it a higher CA. Although

meeting the precondition of ensuring enough fluorine, the oleophobicity of the surface could be improved by enhancing the surface roughness. So, the hexadecane CAs on the polymer treated samples increases from $\sim 121^\circ$ (**S1**) to $\sim 128^\circ$ (**S2**) with the increase of the POSS content in the coating polymer from 0 to 3.2%. However, when the POSS content increases too much, which results in the great decrease of the fluorine content in the coating, the oleophobicity of cotton fabrics becomes poor consequently. The hexadecane CA of **S3** ($\sim 110^\circ$) less than that of **S1** and **S2** could be explained by the fluorine content in the coating polymer for **S3** (35.1%) is much less than that for **S2** (43.4%) and **S1** (44.8%). Based on the influence of the POSS content and fluorine content on the hydrophobicity and oleophobicity of the coated cotton fabric, the hydrophobicity and oleophobicity of the hybrid copolymer can be effectively tuned by varying the feed ratio of POSS.

Flammability of the Coated Fabrics

Limiting oxygen index (LOI) is one of the most commonly used parameters to indicate the flammability of textiles as well as other materials, which is defined as the minimum concentration of oxygen in an oxygen–nitrogen mixture, required to just support downward burning of a vertically mounted test specimen. Hence, higher LOI values represent better flame retardancy. Normal cotton fabric is easily flammable, as a result of its low LOI (18–19%). The LOI of the untreated cotton fabric used in our study is only 18.1%. But when it was coated with **P3**, the LOI of the coated cotton fabric rise to 19.4%. It indicates that incorporation POSS to

TABLE 2 Effect of POSS and Fluorine Content on the Wetting Behaviors of the Coated Fabrics

Samples	Polymer Coated	POSS Ratio (wt %) ^a	Fluorine Ratio (wt %) ^b	Static Contact Angles (°)		
				Water	Salad Oil	Hexadec ^c
S1	P1	0	44.8	133 ± 2	127 ± 2	121 ± 2
S2	P2	3.2	43.4	143 ± 1	132 ± 2	128 ± 4
S3	P3	7.1	35.1	159 ± 2	141 ± 3	110 ± 3

^a POSS ratio was obtained from the elemental analyses of Si.^b Fluorine ratio was obtained from elemental analyses of F.^c Hexade. is an abbreviation for Hexadecane.

the fluoroether-containing polymer could not only improve the water and oil repellency of cotton fabric, but also be helpful to reduce the flammability of the fabric.

In general, when POSS-based nanocomposites heated or combusted, the POSS cage can form the thermally stable ceramic-char surface layer which is able to act as a thermal shield by surface reirradiation and as a barrier to heat or oxygen transfer from flame to the material.^{40,41} Figure 12 shows the SEM images of the residues left after burning the uncoated cotton fabric (a) and **S3** (b,c) in air. The obvious difference between them can be observed. The fabric criss-

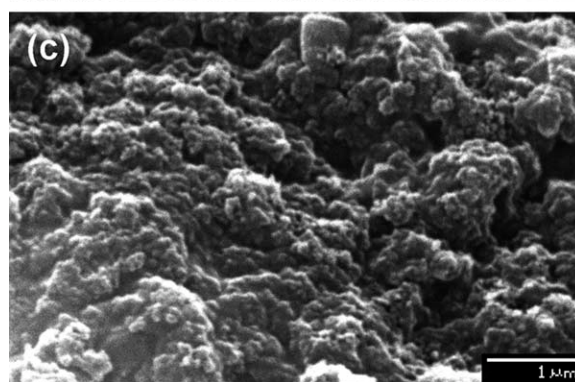
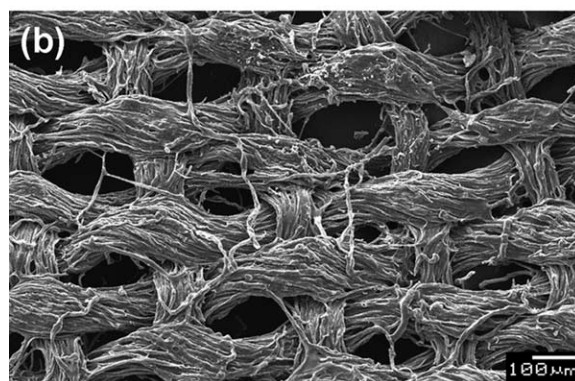
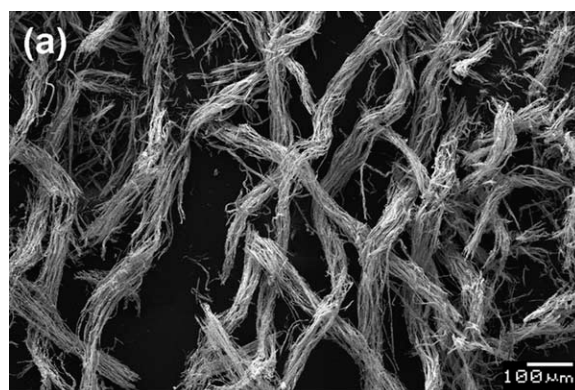
cross networks of the uncoated one are broken, leaving the slim and loose fiber residues [Fig. 12(a)], while **S3** still retain the fibers crisscross network structure [Fig. 12(b)]. In larger magnification scale [Fig. 12(c)], it can be observed



(a)



(b)

FIGURE 11 Photos of the liquids on the cotton fabric treated with **P3** before (a) and after (b).**FIGURE 12** SEM images of the residues of the burned cotton fabric treated with **P3** before (a) and after (b,c).

that on the surface of **S3** residue the bumps and particles appear as a thermally insulating and oxidatively stable silicon oxycarbide surface char.⁴¹

CONCLUSIONS

Well-defined POSS-based fluoroether-containing terpolymer were prepared, characterized, and applied to the cotton fabric as water and oil repellent. The POSS content influences the thermal stability, solubility as well as the structure of the terpolymer. The thermal stability of the terpolymer was improved by POSS incorporation. The structure of the terpolymer with low POSS content is probably to be star-shaped and thus the terpolymer has good solubility. The terpolymer with excessive POSS becomes insoluble due to its crosslinked network structure. More importantly, the hydrophobicity/oleophobicity and the flammability of the coated cotton fabrics also are influenced by the POSS content. When 7.1 wt % POSS incorporated in the resulting terpolymer, the coated cotton fabric shows superhydrophobicity and high oleophobicity. In addition, the terpolymer is potential to be endowed other functional groups from the unreacted vinyl groups in the POSS segments, and thus to be developed for various potential applications.

The National Natural Science Foundation of China (No.21072028) and Shanghai Municipal Scientific Committee (09PJ1400800) are greatly acknowledged for funding this work.

REFERENCES AND NOTES

- Mya, K. Y.; He, C. B.; Huang, J. C.; Xiao, Y.; Dai, J.; Siow, Y. P. *J. Polym. Sci. Part A: Polym. Chem.* **2004**, *42*, 3490–3503.
- Lee, Y. J.; Kuo, S. W.; Huang, C. F.; Chang, F. C. *Polymer* **2006**, *47*, 4378–4386.
- Hussain, H.; Mya, K. Y.; Xiao, Y.; He, C. B. *J. Polym. Sci. Part A: Polym. Chem.* **2008**, *46*, 766–776.
- Liu, L.; Hu, Y.; Song, L.; Nazare, S.; He, S. Q.; Hull, R. *J. Mater. Sci.* **2007**, *42*, 4325–4333.
- Zhao, F.; Huang, Y. D. *Mater. Lett.* **2010**, *64*, 2742–2744.
- Liu, Y. L.; Chang, G. P.; Hsu, K. Y.; Chang, F. C. *J. Polym. Sci. Part A: Polym. Chem.* **2006**, *44*, 3825–3835.
- Strachota, A.; Kroutilova, I.; Kovarova, J.; Matejka, L. *Macromolecules* **2004**, *37*, 9457–9464.
- Huang, C. F.; Kuo, S. W.; Lin, F. J.; Huang, W. J.; Wang, C. F.; Chen, W. Y.; Chang, F. C. *Macromolecules* **2006**, *39*, 300–308.
- Xue, Y. H.; Wang, H. X.; Yu, D. S.; Feng, L. F.; Dai, L. M.; Wang, X. G.; Lin, T. *Chem. Commun.* **2009**, (42), 6418–6420.
- Li, H. Y.; Yu, D. S.; Zhang, J. Y. *Polymer* **2005**, *46*, 5317–5323.
- Wang, J. L.; Ye, Z. B.; Joly, H. *Macromolecules* **2007**, *40*, 6150–6163.
- Zheng, L.; Farris, R. J.; Coughlin, E. B. *J. Polym. Sci. Part A: Polym. Chem.* **2001**, *39*, 2920–2928.
- Fina, A.; Tabuani, D.; Frache, A.; Camino, G. *Polymer* **2005**, *46*, 7855–7866.
- Fina, A.; Tabuani, D.; Camino, G. *Eur. Polym. J.* **2010**, *46*, 14–23.
- Zheng, L.; Kasi, R. M.; Farris, R. J.; Coughlin, E. B. *J. Polym. Sci. Part A: Polym. Chem.* **2002**, *40*, 885–891.
- Hosaka, N.; Otsuka, H.; Hino, M.; Takahara, A. *Langmuir* **2008**, *24*, 5766–5772.
- Choi, M. C.; Hwang, J. C.; Kim, C.; Ando, S.; Ha, C. S. *J. Polym. Sci. Part A: Polym. Chem.* **2010**, *48*, 1806–1814.
- Bharadwaj, R. K.; Berry, R. J.; Farmer, B. L. *Polymer* **2000**, *41*, 7209–7221.
- Ye, Y. S.; Chen, W. Y.; Wang, Y. Z. *J. Polym. Sci. Part A: Polym. Chem.* **2006**, *44*, 5391–5402.
- Iacono, S. T.; Budy, S. M.; Mabry, J. M.; Smith, D. W. *Macromolecules* **2007**, *40*, 9517–9522.
- Tuteja, A.; Choi, W.; Ma, M.; Mabry, J. M.; Mazzella, S. A.; Rutledge, G. C.; McKinley, G. H.; Cohen, R. E. *Science* **2007**, *318*, 1618–1622.
- Xu, J. W.; Li, X.; Cho, C. M.; Toh, C. L.; Shen, L.; Mya, K. Y.; Lu, X. H.; He, C. B. *J. Mater. Chem.* **2009**, *19*, 4740–4745.
- Okano, T.; Kikuchi, A.; Sakurai, Y.; Takei, Y.; Ogata, N. *J. Controlled Release* **1995**, *36*, 125–133.
- Zhang, X.; Shi, F.; Niu, J.; Jiang, Y.; Wang, Z. *J. Mater. Chem.* **2008**, *18*, 621–633.
- Zhang, L.; Zhou, Z.; Cheng, B.; DeSimone, J. M.; Samulski, E. T. *Langmuir* **2006**, *22*, 8576–8580.
- Johansson, A.; Calleja, M.; Dimaki, M. I.; Rasmussen, P.; Boggild, P.; Boisen, A. *Sens. Lett.* **2004**, *2*, 117–120.
- Ellis, D. A.; Mabury, S. A.; Martin, J. W.; Muir, D. C. G. *Nature* **2001**, *412*, 321–324.
- Keil, D. E.; Mehlmann, T.; Butterworth, L.; Peden-Adams, M. M. *Toxicol. Sci.* **2008**, *103*, 77–85.
- Malinverno, G.; Colombo, I.; Visca, M. *Regul. Toxicol. Pharmacol.* **2005**, *41*, 228–239.
- Krupers, M.; Slangen, P. J.; Moller, M. *Macromolecules* **1998**, *31*, 2552–2558.
- Gao, Y.; He, C. L.; Huang, Y. G.; Qing, F. L. *Polymer* **2010**, *51*, 5997–6004.
- He, R.; Toy, P. H.; Lam, Y. *Adv. Synth. Catal.* **2008**, *350*, 54–60.
- Xu, H. Y.; Kuo, S. W.; Lee, J. S.; Chang, F. C. *Macromolecules* **2002**, *35*, 8788–8793.
- Xu, H. Y.; Yang, B. H.; Wang, J. F.; Guang, S. Y.; Li, C. J. *J. Polym. Sci. Part A: Polym. Chem.* **2007**, *45*, 5308–5317.
- Kim, K. M.; Chujo, Y. *J. Polym. Sci. Part A: Polym. Chem.* **2001**, *39*, 4035–4043.
- Liu, Y. L.; Lee, H. C. *J. Polym. Sci. Part A: Polym. Chem.* **2006**, *44*, 4632–4643.
- Wang, R. Y.; Wang, S. F.; Zhang, Y. *J. Appl. Polym. Sci.* **2009**, *113*, 3095–3102.
- Liu, Y. H.; Zheng, S. X. *J. Polym. Sci. Part A: Polym. Chem.* **2006**, *44*, 1168–1181.
- Yang, B. H.; Xu, H. Y.; Wang, J. F.; Gang, S. Y.; Li, C. J. *J. Appl. Polym. Sci.* **2007**, *106*, 320–326.
- S.; Duquesne, S.; Jama, C. *Macromol. Symp.* **2006**, *233*, 180–190.
- Bourbigot, S.; Duquesne, S. *J. Mater. Chem.* **2007**, *17*, 2283–2300.